

$\alpha 2\delta$ -1 couples to NMDA receptors in the hypothalamus to sustain sympathetic vasomotor activity in hypertension

Huijie Ma^{1,2}, Shao-Rui Chen¹, Hong Chen¹, Jing-Jing Zhou¹, De-Pei Li¹  and Hui-Lin Pan¹ 

¹Center for Neuroscience and Pain Research, Department of Anesthesiology and Perioperative Medicine, The University of Texas MD Anderson Cancer Center, Houston, TX, USA

²Department of Physiology, Hebei Medical University, Shijiazhuang, Hebei, China

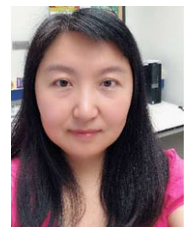
Edited by: Jaideep Bains & Katalin Toth

Key points

- $\alpha 2\delta$ -1 is upregulated, promoting the interaction with NMDA receptors (NMDARs), in the hypothalamus in a rat model of hypertension.
- The prevalence of $\alpha 2\delta$ -1-bound NMDARs at synaptic sites in the hypothalamus is increased in hypertensive animals.
- $\alpha 2\delta$ -1 is essential for the increased presynaptic and postsynaptic NMDAR activity of hypothalamic neurons in hypertension.
- $\alpha 2\delta$ -1-bound NMDARs in the hypothalamus are critically involved in augmented sympathetic outflow in hypertensive animals.

Abstract Increased glutamate NMDA receptor (NMDAR) activity in the paraventricular nucleus (PVN) of the hypothalamus leads to augmented sympathetic outflow in hypertension. However, the molecular mechanisms underlying this effect remain unclear. $\alpha 2\delta$ -1, previously considered to be a voltage-activated calcium channel subunit, is a newly discovered powerful regulator of NMDARs. In the present study, we determined the role of $\alpha 2\delta$ -1 in regulating synaptic NMDAR activity of rostral ventrolateral medulla (RVLM)-projecting PVN neurons in spontaneously hypertensive rats (SHRs). We show that the protein levels of $\alpha 2\delta$ -1 and NMDARs in synaptosomes and the $\alpha 2\delta$ -1–NMDAR complexes in the hypothalamus were substantially higher in SHRs than in normotensive control rats. The basal amplitude of evoked NMDAR currents and NMDAR-mediated synaptic glutamate release in RVLM-projecting PVN neurons were significantly increased in SHRs. Strikingly, inhibiting $\alpha 2\delta$ -1 activity with gabapentin or disrupting the $\alpha 2\delta$ -1–NMDAR association with an $\alpha 2\delta$ -1 C-terminus peptide completely normalized the amplitude of evoked NMDAR currents and NMDAR-mediated synaptic glutamate release in RVLM-projecting PVN neurons in SHRs. In addition, microinjection of the $\alpha 2\delta$ -1 C-terminus peptide into the PVN substantially reduced arterial blood pressure and renal sympathetic nerve

Huijie Ma received her PhD in Physiology from Hebei Medical University in China in 2010 and then continued to study the cardiac protective effect of chronic intermittent hypobaric hypoxia as a faculty member at the same university. She currently works with Dr Hui-Lin Pan as a visiting scientist at The University of Texas MD Anderson Cancer Center in Houston, USA. She is studying the molecular and signalling mechanism governing glutamatergic synaptic plasticity of hypothalamic presympathetic neurons in hypertension. Her general research interest is to define precisely how the central nervous system regulates the sympathetic vasomotor output in cardiovascular disease conditions.



discharges in SHRs. Our findings indicate that $\alpha 2\delta$ -1-bound NMDARs in the PVN are required for the potentiated presynaptic and postsynaptic NMDAR activity of PVN presympathetic neurons and for the elevated sympathetic outflow in hypertension. $\alpha 2\delta$ -1-bound NMDARs may be an opportune target for treating neurogenic hypertension.

(Received 1 May 2018; accepted after revision 29 June 2018; first published online 3 July 2018)

Corresponding author H.-L. Pan: Department of Anesthesiology and Perioperative Medicine, Unit 110, The University of Texas MD Anderson Cancer Center, 1515 Holcombe Blvd, Houston, TX 77030, USA. Email: huilinpan@mdanderson.org

Introduction

Almost half of adults in the USA are considered as having high blood pressure in accordance with new guidelines from the American Heart Association and the American College of Cardiology (Reboussin *et al.* 2017). Hypertension is a well-recognized risk factor for coronary artery disease, kidney failure and stroke. Essential hypertension, or hypertension of unknown cause, which accounts for more than 90% of cases of hypertension, results from a complex interaction of genetic and environmental factors. Major pathophysiological mechanisms of hypertension include activation of the sympathetic nervous system and the renin–angiotensin–aldosterone system, endothelial dysfunction, increased vascular reactivity, and vascular remodelling (Oparil *et al.* 2003; DiBona, 2013). The hypothalamic paraventricular nucleus (PVN) neurons that project to the rostral ventrolateral medulla (RVLM) and intermediolateral cell column in the spinal cord play a pivotal role in the augmented sympathetic outflow in spontaneously hypertensive rats (SHRs) (Allen, 2002; Li & Pan, 2007). Although increased glutamate NMDA receptor (NMDAR) activity in the PVN leads to elevated sympathetic vasomotor activity in hypertension (Li & Pan, 2007; Li *et al.* 2008; Qiao *et al.* 2017), the molecular mechanisms underlying synaptic NMDAR hyperactivity of PVN presympathetic neurons remain unclear.

$\alpha 2\delta$ -1 was initially known as a subunit of voltage-activated Ca^{2+} channels (VACCs). $\alpha 2\delta$ -1 is also the binding site of gabapentinoids, including gabapentin and pregabalin (Gee *et al.* 1996; Marais *et al.* 2001; Fuller-Bicer *et al.* 2009), which are often used for treating neuropathic pain. However, gabapentinoids have little effect on VACC activity (Rock *et al.* 1993; Schumacher *et al.* 1998; Chen *et al.* 2018). We recently discovered that $\alpha 2\delta$ -1 interacts with NMDARs in the spinal cord and promotes NMDAR synaptic trafficking in neuropathic pain (Chen *et al.* 2018). Interestingly, $\alpha 2\delta$ -1 is highly expressed in the hypothalamus, particularly in the PVN (Cole *et al.* 2005; Taylor & Garrido, 2008). Nevertheless, nothing is known about the involvement of $\alpha 2\delta$ -1 in regulating NMDAR activity in the PVN and sympathetic outflow in hypertension.

In the present study, we demonstrate that $\alpha 2\delta$ -1 forms a protein complex with NMDARs and plays an essential role

in the increased presynaptic and postsynaptic NMDAR activity in PVN presympathetic neurons and augmented sympathetic outflow in SHRs. The results of the present study provide new insight into the molecular mechanisms underlying the elevation of sympathetic vasomotor tone in hypertension.

Methods

Ethical approval and animal models

The experimental procedures and protocols were approved by the Institutional Animal Care and Use Committee of The University of Texas MD Anderson Cancer Center (approval ref. no. 919-RN02) and conformed with the National Institutes of Health guidelines on the ethical use of animals. Thirteen-week-old male normotensive Wistar-Kyoto (WKY) rats and spontaneously hypertensive rats (SHRs) (Harlan, Indianapolis, IN, USA) were used for most of the experiments. Blood pressure was measured before the electrophysiological experiments via a non-invasive tail-cuff system (IITC Life Science, Inc., Woodland Hills, CA, USA) to confirm hypertension in a randomly selected group of adult SHRs and WKY rats (Table 1).

Immunoblotting

Rats were anaesthetized with 2–3% isoflurane and then decapitated. The brain was quickly removed and placed in ice-cold artificial CSF (aCSF) saturated with 95% O_2 and 5% CO_2 . Hypothalamic slices were sectioned

Table 1. Arterial blood pressure of 13-week-old WKY rats and SHRs

	WKY	SHR
SAP	108.7 ± 2.88	178.57 ± 2.38***
DAP	75.57 ± 2.11	126.09 ± 2.57***
MAP	86.61 ± 2.10	143.58 ± 2.16***

Blood pressure was measured using a tail-cuff system. SAP, systolic blood pressure; DAP, diastolic blood pressure; MAP, mean arterial blood pressure. WKY rats, $n = 30$ rats; SHRs, $n = 35$ rats. *** $P < 0.001$ compared to the WKY group.

1.08–2.12 mm caudal to the bregma, and hypothalamic tissues containing the PVN were micropunched bilaterally with a slice punch (0.5 mm diameter) following stereotactic co-ordinates: 0.5 mm lateral to the midline and 6.5–9.0 mm ventral to the surface of the cortex (Ye *et al.* 2012b; Qiao *et al.* 2017). The tissues were frozen in liquid nitrogen and then transferred to a freezer at -80°C .

Total proteins were extracted with a RIPA lysis/extraction buffer (Thermo Fisher Scientific, Waltham, MA, USA) in the presence of a mixture containing protease inhibitor cocktail (Sigma-Aldrich, St Louis, MO, USA). The PVN tissues were homogenized and then subjected to centrifugation at 16,000 g for 10 min to obtain the supernatant. For synaptosome isolation, the hypothalamic tissues (pooled from two rats per sample) were homogenized using 10 volumes of ice-cold Hepes-buffered sucrose solution (0.32 mol L⁻¹ sucrose, 1 mmol L⁻¹ EGTA and 4 mmol L⁻¹ Hepes at pH, 7.4) containing the protease inhibitor cocktail. The homogenates were centrifuged at 2000 g for 10 min at 4°C to remove the nuclei and large debris. The supernatant was centrifuged at 20,000 g for 30 min to obtain the crude synaptosomes. The synaptosomal pellets were subjected to lysis via hypoosmotic shock in nine volumes of ice-cold Hepes buffer with the protease inhibitor cocktail for 30 min. The lysates were centrifuged at 25,000 g for 45 min at 4°C to obtain the synaptosomal fraction (Chen *et al.* 2018), which was then dissolved in sodium dodecyl sulphate sample buffer at a final concentration of 0.25 $\mu\text{g } \mu\text{L}^{-1}$ for immunoblotting. The protein concentration was determined by bicinchoninic acid assay.

The samples were subjected to 4–15% Tris-HCl SDS-PAGE (#456-1086; Bio-Rad, Hercules, CA, USA) and then transferred to a polyvinylidene difluoride membrane (EMD Millipore, Burlington, MA, USA). The membranes were treated with 5% non-fat dry milk in Tris-buffered saline solution at 25°C for 1 h, and then incubated in Tris-buffered saline solution supplemented with 0.1% Triton X-100, 1% BSA and rabbit anti-GluN1 (#G8913; dilution 1:2000; Sigma-Aldrich), rabbit anti- $\alpha 2\delta$ -1 (#C0515; dilution 1:500; Sigma-Aldrich), rabbit anti-GAPDH antibody (#ab37168; dilution 1:1000; Abcam, Cambridge, MA, USA) or mouse anti-PSD-95 (#75-348; dilution 1:1000; NeuroMab, Davis, CA, USA) antibody overnight at 4°C. The membrane was washed three times and then incubated with horseradish peroxidase-conjugated anti-rabbit or anti-mouse IgG antibody (dilution 1:7500; Jackson ImmunoResearch, West Grove, PA, USA) for 1 h at room temperature. An ECL kit (Thermo Fisher Scientific) was used to detect the protein band, which was visualized and quantified with the Odyssey Fc Imager (LI-COR Biosciences, Lincoln, NE, USA) and normalized to the

GAPDH or PSD-95 (a synaptic protein) band on the same blot.

Co-immunoprecipitation

Rat hypothalamic slices containing the PVN were sectioned 1.08–2.12 mm caudal to the bregma. The tissues were dissected and homogenized in ice-cold IP lysis buffer (#87788; Thermo Fisher Scientific; 25 mmol L⁻¹ Tris-HCl, pH 7.4, 150 mmol L⁻¹ NaCl, 1% NP-40, 1 mmol L⁻¹ EDTA, 5% glycerol and the protease inhibitor cocktail) and incubated on ice for 30 min for total protein preparation. The lysates were centrifuged for 15 min at 16,000 g to obtain the supernatants. The protein sample were quantified and incubated at 4°C overnight with Protein G beads (#16-266; EMD Millipore) prebound to rabbit anti-GluN1 antibody (#G8913; dilution 1:100; Sigma-Aldrich). Protein G beads prebound to rabbit IgG were used as controls. Samples were washed three times with immunoprecipitation buffer and then immunoblotted with mouse anti- $\alpha 2\delta$ -1 antibody (#sc-271697; dilution 1:500; Santa Cruz Biotechnology, Santa Cruz, CA, USA). The protein bands were detected using immunoblotting analysis.

Retrograde labelling of RVLM-projecting PVN presympathetic neurons

We performed retrograde labelling to identify RVLM-projecting PVN neurons as described previously (Li & Pan, 2006; Qiao *et al.* 2017). The rats were anaesthetized with 2–3% isoflurane and placed in a stereotactic frame. A small piece of skull was removed and a microinjection pipette (tip diameter, 20–30 μm) filled with fluorescent microsphere suspension (FluoSpheres, 0.04 μm ; Molecular Probes, Invitrogen, Eugene, OR, USA) was advanced into the RVLM in accordance with the stereotactic co-ordinates: 12.5–13.0 mm caudal to the bregma, 1.9–2.0 mm lateral to the midline and 7.5–8.0 mm ventral to the dura. The FluoSpheres were pressure-injected (Nanoject II Microinjectors; Drummond Scientific Company, Broomall, PA, USA) into the RVLM bilaterally in two separate 50 nL injections using a micromanipulator. The tracer injection was monitored through a surgical microscope. The rats were returned to their home cages for 3–5 days to allow the FluoSpheres to be transported into the PVN. The animals were inspected daily for motor activity, signs of infection, and food and water intake.

Brain slice preparation

The rats were rapidly decapitated under 2–3% isoflurane anaesthesia. The brain was quickly removed

and sliced in an ice-cold aCSF solution containing (in mmol L⁻¹) 126 NaCl, 3 KCl, 1.5 MgCl₂, 2.4 CaCl₂, 1.2 NaH₂PO₄, 10 glucose and 26 NaHCO₃ saturated with 95% O₂ and 5% CO₂. Coronal hypothalamic slices (300 μm thick) containing the PVN were obtained from FluoSphere-injected rats using a vibrating microtome (VT1000 S; Leica Biosystems Inc., Buffalo Grove, IL, USA). The slices were incubated in the aCSF at 34°C for at least 1 h before recording. To confirm the injection sites of the FluoSpheres, the RVLN was sectioned at the injection level and viewed under a microscope immediately after the rat was killed. Data were excluded from the analysis if either of the injection sites were not located within the RVLN.

Electrophysiological recordings

The labelled PVN neurons were identified under an upright microscope (BX51WI; Olympus, Tokyo, Japan) with epifluorescence and infrared differential interference contrast optics. Whole-cell, patch clamp recordings were performed in FluoSphere-labelled PVN neurons. The hypothalamic slices were continuously perfused with aCSF (saturated by 95% O₂ and 5% CO₂; speed, 3.0 mL min⁻¹) at 34°C maintained by an inline solution heater.

The miniature EPSCs (mEPSCs) were recorded in the presence of 1 μmol L⁻¹ tetrodotoxin and 20 μmol L⁻¹ bicuculline at a holding potential of -60 mV (Li *et al.* 2003; Ye *et al.* 2011). The recording glass pipette (4–8 MΩ) was filled with internal solution containing (in mmol L⁻¹) 135.0 potassium gluconate, 5.0 tetraethylammonium, 2.0 MgCl₂, 0.5 CaCl₂, 5.0 HEPES, 5.0 EGTA, 5.0 Mg-ATP and 0.5 Na-GTP (adjusted to pH 7.2–7.4 with 1 mol L⁻¹ KOH; 290–300 mosmol L⁻¹). A sodium channel blocker, lidocaine *N*-ethyl bromide (10.0 mmol L⁻¹), was included in the pipette solution to block the firing activity of the recorded neuron.

The evoked EPSCs were elicited by electrical stimulation (0.2 ms, 0.8–1.0 mA at 0.2 Hz) through a bipolar tungsten electrode connected to a stimulator. The tip of the stimulation electrode was placed on the ventral side 150 μm from the recorded neuron (Li *et al.* 2003; Li *et al.* 2005). The internal solution contained (in mmol L⁻¹): 110.0 Cs₂SO₄, 2.0 MgCl₂, 0.1 CaCl₂, 10.0 HEPES, 1.1 EGTA, 0.3 Na₂-GTP and 2.0 Mg-ATP, adjusted to pH 7.25 with 1.0 mol L⁻¹ CsOH (270–290 mosm). Evoked α-amino-3-hydroxy-5-methyl-4-isoxazolepropionic acid receptor (AMPA)-EPSCs were recorded at a holding potential of -60 mV in the presence of 10 μmol L⁻¹ bicuculline, and evoked NMDAR-EPSCs were recorded at a holding potential of +40 mV in the presence of 10 μmol L⁻¹ bicuculline and 10 μmol L⁻¹ 6,7-dinitroquinoxaline-2,3-dione. We have shown that the evoked NMDAR-EPSCs at +40 mV were abolished by the NMDAR specific antagonist, AP5, whereas the evoked

AMPA-EPSCs at -60 mV were completely blocked by the AMPAR antagonist 6,7-dinitroquinoxaline-2,3-dione (Li *et al.* 2003; Li *et al.* 2008; Ye *et al.* 2011). The amplitude of AMPAR-EPSCs recorded in labelled PVN neurons at a holding potential of -60 mV is similar in WKY rats and SHR rats (Li *et al.* 2017). Therefore, AMPAR-EPSCs were used to normalize the NMDAR-EPSCs elicited under the same stimulation intensity (0.8 mA) in the present study.

To record postsynaptic NMDAR currents, we puffed NMDA (100 μmol L⁻¹) directly onto the recorded neuron at a holding potential of -60 mV using a positive pressure system (4 psi, 50 ms; Toohey Company, Fairfield, NJ, USA). The puff pipette (10 μm tip diameter) was placed 150 μm away from the recorded neuron. Because NMDARs are voltage-dependently blocked by Mg²⁺ at a negative holding potential and co-activated by glycine, puff NMDA-induced currents were recorded in Mg²⁺-free aCSF in the presence of 10 μmol L⁻¹ glycine and 1 μmol L⁻¹ tetrodotoxin. Although puff application of NMDA can also result in presynaptic release of glutamate, the currents elicited by presynaptic glutamate release are very small and negligible compared to currents produced by a large amount of puff glutamate receptor agonists. Therefore, the current elicited by puff application of NMDA is generally considered to be a measure of postsynaptic NMDAR activity (Li *et al.* 2008; Ye *et al.* 2011).

PVN microinjection and recording of renal sympathetic nerve activity

Rats were anaesthetized via i.p. administration of a mixture of α-chloralose (60 mg kg⁻¹) and urethane (800 mg kg⁻¹) and mechanically ventilated with trachea cannulation. The arterial blood pressure (ABP) was monitored via a catheter placed in the left femoral artery, and heart rate (HR) was extracted from the pulsatile pressure wave. A retroperitoneal incision was made, and a branch of the left renal postganglionic sympathetic nerve was isolated under a surgical microscope. The renal sympathetic nerve was cut distally to ensure that afferent activity was not recorded. The ABP, HR and renal sympathetic nerve activity (RSNA) were recorded using a 1401-PLUS analogue-to-digital converter and Spike2 system (Cambridge Electronic Design, Cambridge, UK). After the brain was exposed, a microinjection pipette (tip diameter 20–30 μm) was advanced into the PVN in accordance with the stereotactic co-ordinates: 1.6–2.0 mm caudal to the bregma, 0.5 mm lateral to the midline and 7.0–7.5 mm ventral to the dura. The microinjection was performed using a Nanoject II (Drummond Scientific Company) and monitored using a surgical microscope as described previously (Li & Pan, 2006, 2007; Qiao *et al.* 2017). AP5 (1.0 nmol, 50 nL) was microinjected into the PVN to observe the change in ABP and RSNA in the presence of α2δ-1Tat peptide

(50 pmol, 50 nL; Bio Basic, Markham, Ontario, Canada) or Tat-fused control peptide (50 pmol, 50 nL). At the end of each experiment, the electrical background noise was measured after the proximal end of renal nerve was crushed at the end of each experiment. To determine the location of the injection site and diffusion of the drugs in the PVN, we included 5% rhodamine-labelled fluorescent microspheres (0.04 μ m; Molecular Probes) in the injection solution (Li & Pan, 2006, 2007; Qiao *et al.* 2017). Rats were excluded from the data analysis if the microinjections were misplaced outside the PVN.

Celiac ganglionectomy and ABP measurement using telemetry

Celiac ganglionectomy (CGx) or sham surgery was performed aseptically in SHRs anaesthetized with 2–3% isoflurane as described previously (Ye *et al.* 2011; Qiao *et al.* 2017). The celiac ganglion area was exposed through a midline laparotomy and identified within the area near the superior mesenteric artery and celiac artery (Hamer & Santer, 1981). For rats undergoing CGx, the celiac plexus and all visible nerves were dissected and removed as completely as possible. In sham control rats, the celiac ganglion plexus was exposed but not disrupted. A Millar catheter (Millar, Houston, TX, USA) attached to the transmitter was inserted into the abdominal aorta for continuous monitoring of ABP, and the transmitter body was implanted in an abdominal cavity. The rats were housed individually, and the ABP was measured in freely moving rats by using a telemetry system (Telemetry Research Ltd., Houston, TX, USA) (Ye *et al.* 2011; Ye *et al.* 2012a). The ABP data were recorded continuously after surgery and analysed with a data acquisition system (LabChart; AD Instruments, Sydney, Australia). Two weeks after CGx or sham surgery, the rats were anaesthetized with 2–3% isoflurane and then decapitated. The brain tissues of rats were harvested for immunoblotting analysis.

Statistical analysis

For electrophysiological recording experiments, only one neuron in each brain slice was recorded, and at least four animals were used for each recording protocol. Data are presented as the mean \pm SEM. The amplitude and frequency of mEPSCs were analysed offline with peak detection software (MiniAnalysis; Synaptosoft Inc., Decatur, GA, USA). The cumulative probabilities of the amplitude and inter-event interval were compared using the Kolmogorov–Smirnov test. Clampfit, version 10.2 (Molecular Devices, Sunnyvale, CA, USA) was used to determine the peak amplitude of evoked EPSCs and

puff NMDA currents. The mean ABP, RSNA and HR were analysed using Spike2 software. The mean ABP was derived from the pulsatile ABP and calculated as the diastolic pressure plus one-third of the pulse pressure. RSNA was rectified and integrated offline after subtracting the background noise, which was recorded after the proximal end of renal nerve was crushed at the end of each experiment. The integrated RSNA value was calculated and derived from the raw RSNA with an integrating time of 1.0 s using Spike2 software. Control values were obtained by averaging the signal over a 60 s period immediately before PVN microinjection. Response values after each intervention were averaged over 30 s when the maximal responses occurred. A two-tailed Student's *t* test was used to compare two groups and one-way ANOVA followed by the Dunnett's and Tukey's *post hoc* tests was used to compare more than two groups. Statistical analyses were performed using Prism, version 7 (GraphPad Software Inc., La Jolla, CA). $P < 0.05$ was considered statistically significant.

Results

$\alpha 2\delta$ -1 is upregulated in the PVN in SHRs

We used immunoblotting to determine the $\alpha 2\delta$ -1 protein levels in the PVN in WKY rats and SHRs. The $\alpha 2\delta$ -1 protein level in the PVN was significantly greater in SHRs than in WKY rats ($P = 0.0074$, $t_{12} = 3.217$, $n = 7$ rats in each group) (Fig. 1A).

To determine whether the higher $\alpha 2\delta$ -1 protein level in the PVN of SHRs was secondary to elevated ABP in SHRs, we performed CGx (Ye *et al.* 2011; Qiao *et al.* 2017) to lower ABP in SHRs and then measured $\alpha 2\delta$ -1 protein levels in their PVNs. CGx substantially lowered ABP in SHRs, as measured by radio telemetry, compared to the sham group ($n = 6$ rats in each group) (Fig. 1B). Immunoblotting showed that lowering ABP did not significantly alter the $\alpha 2\delta$ -1 protein level in the PVN in SHRs (Fig. 1C). In addition, the $\alpha 2\delta$ -1 protein level in the PVN was significantly higher in 4-week-old SHRs than in age-matched WKY rats ($P = 0.027$, $t_{10} = 2.584$, $n = 6$ rats in each group) (Fig. 1D). These data suggest that $\alpha 2\delta$ -1 upregulation in the PVN in SHRs is independent of ABP changes.

$\alpha 2\delta$ -1 physically interacts with NMDARs in the hypothalamus in SHRs

We recently showed that $\alpha 2\delta$ -1 physically interacts with NMDARs in the spinal cord (Chen *et al.* 2018). To determine whether $\alpha 2\delta$ -1 and NMDARs interact in the hypothalamus, we conducted co-immunoprecipitation

analyses using total proteins extracted from the PVN of SHRs and WKY rats. The anti-GluN1 antibody co-precipitated with $\alpha 2\delta$ -1 in the hypothalamic tissues obtained from these rats, whereas the irrelevant IgG did not co-precipitate with $\alpha 2\delta$ -1 (Fig. 1E). Furthermore, the $\alpha 2\delta$ -1–GluN1 complex level in the hypothalamus was much higher in SHRs than in WKY rats ($P = 0.0204$, $t_{10} = 2.752$, $n = 6$ rats in each group) (Fig. 1E). These results indicate that $\alpha 2\delta$ -1 forms a protein complex in the hypothalamus and that the $\alpha 2\delta$ -1–NMDAR interaction is enhanced in SHRs.

Synaptic $\alpha 2\delta$ -1-bound NMDARs are increased in the hypothalamus in SHRs

$\alpha 2\delta$ -1 primarily increases NMDAR activity by promoting synaptic targeting of NMDARs in the spinal cord after nerve injury (Chen *et al.* 2018). We next determined whether $\alpha 2\delta$ -1–NMDAR complexes are increased at synaptic sites in the hypothalamus of SHRs. Immunoblotting of isolated synaptosomes showed that the protein levels of both $\alpha 2\delta$ -1 ($P = 0.0009$, $t_{10} = 4.655$) and GluN1 ($P = 0.0189$, $t_{10} = 2.797$), an obligatory subunit of NMDARs, were much higher in SHRs than in WKY rats

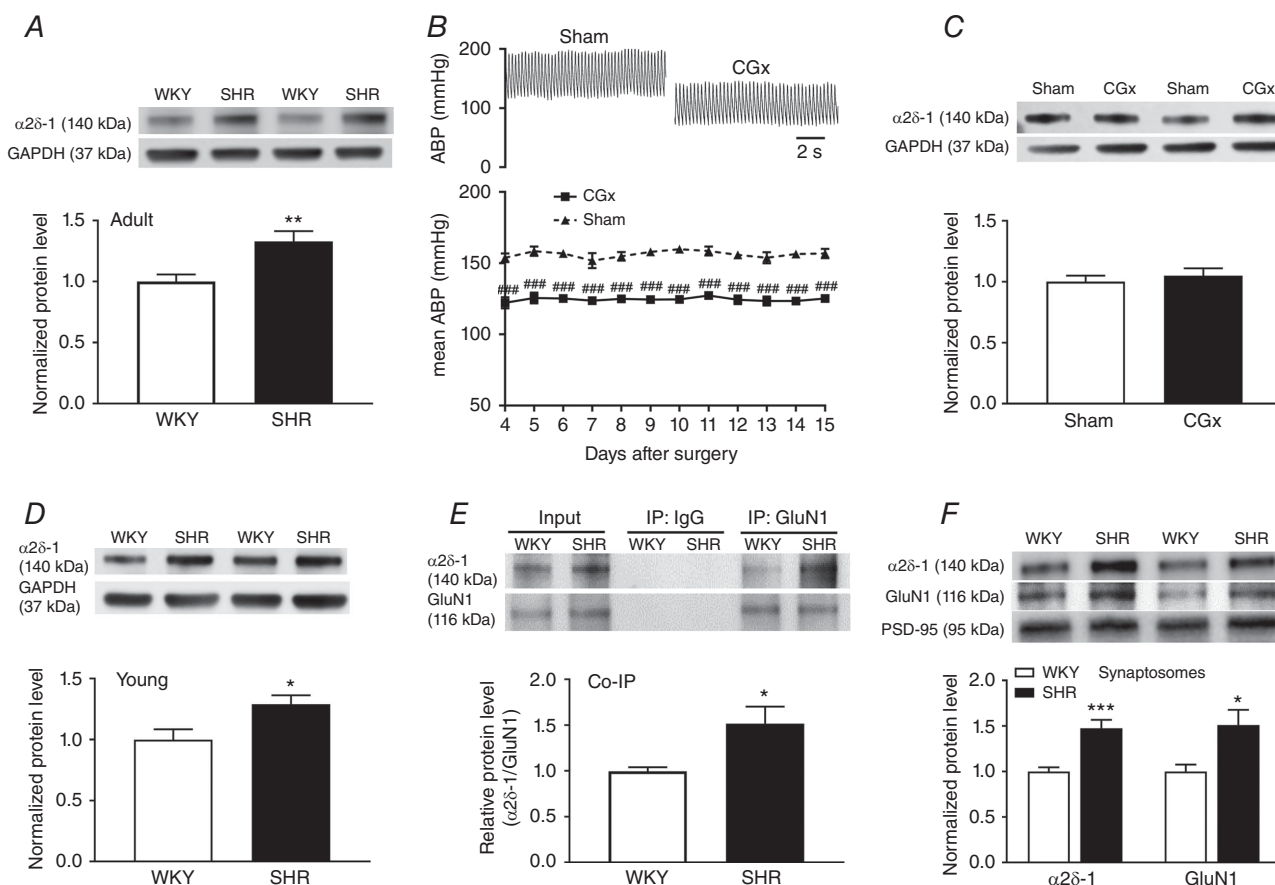


Figure 1. $\alpha 2\delta$ -1 interacts with NMDARs in the hypothalamus and increases the synaptic expression of $\alpha 2\delta$ -1-bound NMDARs in SHRs

A, representative blot images and mean changes show the $\alpha 2\delta$ -1 protein level in the PVN in adult WKY rats and SHRs ($n = 7$ rats per group). B, original ABP traces and summary data show the effect of CGx or sham surgery on the mean ABP in SHRs ($n = 6$ rats in each group). C, original blot images and summary data show the $\alpha 2\delta$ -1 levels (normalized to GAPDH) in the PVN in SHRs subjected to CGx or sham surgery ($n = 6$ rats in each group). D, representative blot images and mean changes show the $\alpha 2\delta$ -1 protein level in the PVN in young WKY rats and SHRs ($n = 6$ rats per group). E, representative blot images and co-immunoprecipitation analysis show the interaction between $\alpha 2\delta$ -1 and GluN1 in total protein extracts of hypothalamic tissues from WKY rats and SHRs ($n = 6$ independent experiments per group, each tissue sample was pooled from two rats). Proteins were immunoprecipitated first with an anti-GluN1 antibody or IgG and then immunoblotted using an anti- $\alpha 2\delta$ -1 antibody. F, original blot images and quantification data show the protein levels of $\alpha 2\delta$ -1 and GluN1 (normalized to PSD-95, a synaptic protein) in hypothalamic synaptosomes in WKY rats and SHRs ($n = 6$ independent experiments per group, each tissue sample was pooled from two rats). * $P < 0.05$, ** $P < 0.01$, *** $P < 0.001$ compared to the sham group. ### $P < 0.001$ compared to the sham group.

($n = 6$ independent experiments, each tissue sample was pooled from two rats) (Fig. 1F). These data suggest that the prevalence of $\alpha 2\delta$ -1-bound NMDARs at the synaptic site in the hypothalamus is increased in SHR.

$\alpha 2\delta$ -1 is indispensable for enhanced postsynaptic NMDAR activity of PVN presympathetic neurons in SHRs

We then determined whether $\alpha 2\delta$ -1 plays a role in regulating synaptic NMDAR activity of RVLM-projecting PVN neurons in SHRs. We treated the hypothalamic slices from WKY rats and SHRs with either vehicle (aCSF) or gabapentin ($100 \mu\text{mol L}^{-1}$), an $\alpha 2\delta$ -1-inhibitory ligand (Gee *et al.* 1996; Fuller-Bicer *et al.* 2009), for 60 min before electrophysiological recording. The amplitude of evoked NMDAR-EPSCs of labelled RVLM-projecting PVN neurons was significantly larger in SHRs ($n = 8$ neurons) than in WKY rats ($n = 9$ neurons) ($P < 0.0001$, $F_{3,30} = 25.69$) (Fig. 2A–C). Gabapentin treatment completely normalized the amplitude of evoked NMDAR-EPSCs of labelled PVN neurons in SHRs but had no effect in WKY rats (Fig. 2B and C). By contrast, gabapentin did not significantly alter the amplitude of evoked AMPAR-EPSCs of labelled PVN neurons in WKY rats or SHRs. The ratio of NMDAR-EPSCs to AMPAR-EPSCs in vehicle-treated slices was significantly higher in SHRs than in WKY rats (WKY, $n = 9$ neurons; SHR, $n = 8$ neurons; $P < 0.0001$, $F_{3,30} = 26.52$) (Fig. 2B–D). Gabapentin treatment also restored the ratio of NMDAR-EPSCs to AMPAR-EPSCs in SHRs to the level in WKY rats, although it had no such effect in WKY rats (Fig. 2B–D).

To directly determine the role of $\alpha 2\delta$ -1 in increased postsynaptic NMDAR activity of PVN presympathetic neurons in SHRs, we examined the effect of gabapentin on NMDAR currents elicited by puff application of NMDA ($100 \mu\text{mol L}^{-1}$) directly to labelled PVN neurons. In vehicle-treated slices, puff NMDA induced a significantly larger current of labelled neurons in SHRs than in WKY rats (WKY, $n = 11$ neurons; SHR, $n = 12$ neurons; $P < 0.0001$, $F_{3,41} = 20.68$) (Fig. 2E and F). Treatment with gabapentin completely restored the puff NMDA currents of labelled PVN neurons in SHRs to the levels in WKY rats (Fig. 2E and F). These results suggest that $\alpha 2\delta$ -1 is critically involved in increased postsynaptic NMDAR activity of PVN presympathetic neurons in SHRs.

$\alpha 2\delta$ -1-bound NMDARs are essential for increased postsynaptic NMDAR activity of PVN presympathetic neurons in SHRs

The C-terminus of $\alpha 2\delta$ -1 is essential for its interaction with NMDARs, and a 30-amino-acid

peptide (VSGLNPSLWSIFGLQFILLWLVSGRHYLW) mimicking the transmembrane C-terminus of $\alpha 2\delta$ -1 fused with Tat protein (YGRKKRRQRRR; $\alpha 2\delta$ -1Tat peptide) effectively interrupts the $\alpha 2\delta$ -1–NMDAR interaction (Chen *et al.* 2018). Pre-treatment with a Tat-fused scrambled control peptide (FGLGWQPWSLSFYLVWVSGILSLVHLIRSN, $1 \mu\text{mol L}^{-1}$, 60 min) did not affect the evoked AMPAR-EPSCs, evoked NMDAR-EPSCs or the ratio of NMDAR-EPSCs to AMPAR-EPSCs of labelled PVN neurons from WKY rats ($n = 10$ neurons) or SHRs ($n = 9$ neurons) (Fig. 3A–C). By contrast, $\alpha 2\delta$ -1Tat peptide ($1 \mu\text{mol L}^{-1}$, 60 min) fully normalized the amplitude of evoked NMDAR-EPSCs of labelled PVN neurons in SHRs ($n = 9$ neurons in each group) (Fig. 3A and B). However, $\alpha 2\delta$ -1Tat peptide had no effect on the amplitude of evoked NMDAR-EPSCs of labelled PVN neurons in WKY rats (Fig. 3A and B). Also, $\alpha 2\delta$ -1Tat peptide had no effect on the amplitude of evoked AMPAR-EPSCs of labelled PVN neurons in WKY rats or SHRs (Fig. 3A and B). $\alpha 2\delta$ -1Tat peptide normalized the ratio of NMDAR-EPSCs to AMPAR-EPSCs in SHRs to the level in WKY rats (Fig. 3C), although it had no effect on the ratio of NMDAR-EPSCs to AMPAR-EPSCs in WKY rats.

Furthermore, treatment with $\alpha 2\delta$ -1Tat peptide had no effect on the amplitude of puff NMDA currents in WKY rats. However, $\alpha 2\delta$ -1Tat peptide restored the amplitude of puff NMDA currents of labelled PVN neurons in SHRs ($n = 11$ neurons) to the level in WKY rats ($n = 8$ neurons) (Fig. 3D and E). By contrast, treatment with the Tat-fused control peptide had no effect on the amplitude of puff NMDA currents in WKY ($n = 8$ neurons) or SHRs ($n = 11$ neurons) (Fig. 3D and E). These data indicate that $\alpha 2\delta$ -1-bound NMDARs are crucial for increased postsynaptic NMDAR activity of PVN presympathetic neurons in SHRs.

$\alpha 2\delta$ -1 is required for tonic activation of presynaptic NMDARs of PVN presympathetic neurons in SHRs

Presynaptic NMDARs in the PVN are normally latent, although they are tonically activated to augment glutamate release from presynaptic terminals in SHRs (Li *et al.* 2008; Li *et al.* 2017; Qiao *et al.* 2017). To determine whether $\alpha 2\delta$ -1 contributes to increased presynaptic NMDAR activity in the PVN in SHRs, we recorded mEPSCs, which reflect quantal release of glutamate from presynaptic terminals (Sulzer & Pothos, 2000). The baseline frequency of mEPSCs of labelled PVN neurons was significantly higher in SHRs than in WKY rats (WKY, $n = 10$ neurons; SHR, $n = 11$ neurons; $P = 0.0012$, $F_{5,57} = 6.607$) (Fig. 4), whereas the amplitude of mEPSCs did not differ significantly between the two groups. To

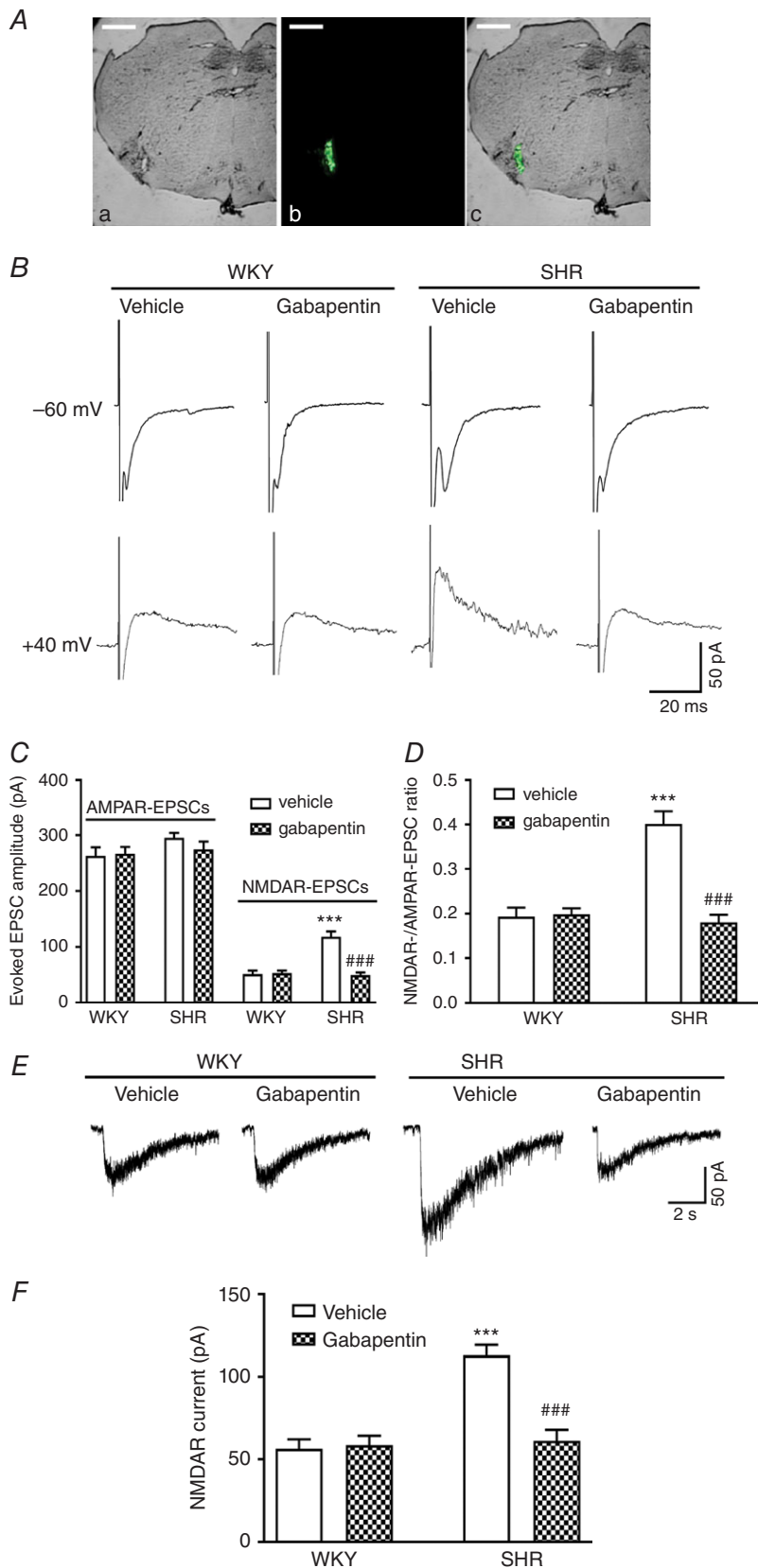


Figure 2. $\alpha 2\delta$ -1 is required for increased postsynaptic NMDAR activity of RVLM-projecting PVN neurons in SHRs

A, representative images show the microinjection site in the RVLM in bright-field (**Aa**), fluorescence (**Ab**) and overlay images (**Ac**) from the same tissue section. Scale bar = 1 mm. **B**, representative current traces of evoked AMPAR-EPSCs (at -60 mV) and NMDAR-EPSCs (at $+40$ mV) recorded in a labelled PVN neuron treated with vehicle or $100 \mu\text{mol L}^{-1}$ gabapentin in slices obtained from a WKY rat and an SHR. **C** and **D**, summary of evoked AMPAR-EPSC and NMDAR-EPSC data (**C**) and the ratio of NMDAR-EPSCs to AMPAR-EPSCs (**D**) in labelled PVN neurons pretreated with vehicle or gabapentin in slices from WKY rats ($n = 9$ neurons in each group) or SHRs ($n = 8$ neurons in each group). **E** and **F**, original current traces (**E**) and summary data (**F**) show the effect of $100 \mu\text{mol L}^{-1}$ gabapentin on puff NMDA ($100 \mu\text{mol L}^{-1}$) elicited currents of labelled PVN neurons recorded from WKY rats ($n = 11$ neurons in each group) and SHRs (vehicle, $n = 12$ neurons; gabapentin, $n = 11$ neurons). $***P < 0.001$ compared to the WKY + vehicle group. $###P < 0.001$ compared to the SHR + vehicle group. [Colour figure can be viewed at wileyonlinelibrary.com]

confirm that the increase in the frequency of mEPSCs in SHRs is mediated by NMDARs, we bath-applied a specific NMDAR antagonist, AP5 ($50 \mu\text{mol L}^{-1}$). AP5 application readily normalized the frequency of mEPSCs of labelled PVN neurons in SHRs to the level in WKY rats (Fig. 4C–E), whereas it had no effect in WKY rats (Fig. 4A–E). Gabapentin ($100 \mu\text{mol L}^{-1}$, 60 min) treatment fully restored the baseline frequency of mEPSCs of labelled PVN neurons in SHRs without changing their

amplitude ($n = 11$ neurons) (Fig. 4D–F). Subsequent bath application of AP5 no longer had any effect on the frequency of mEPSCs of labelled PVN neurons in SHR brain slices pretreated with gabapentin. By contrast, gabapentin had no effect on the frequency or amplitude of mEPSCs of labelled PVN neurons in WKY rats (Fig. 4B, E and F). These findings suggest that $\alpha 2\delta$ -1 is obligatory for tonic activation of presynaptic NMDARs of PVN presympathetic neurons in SHRs.

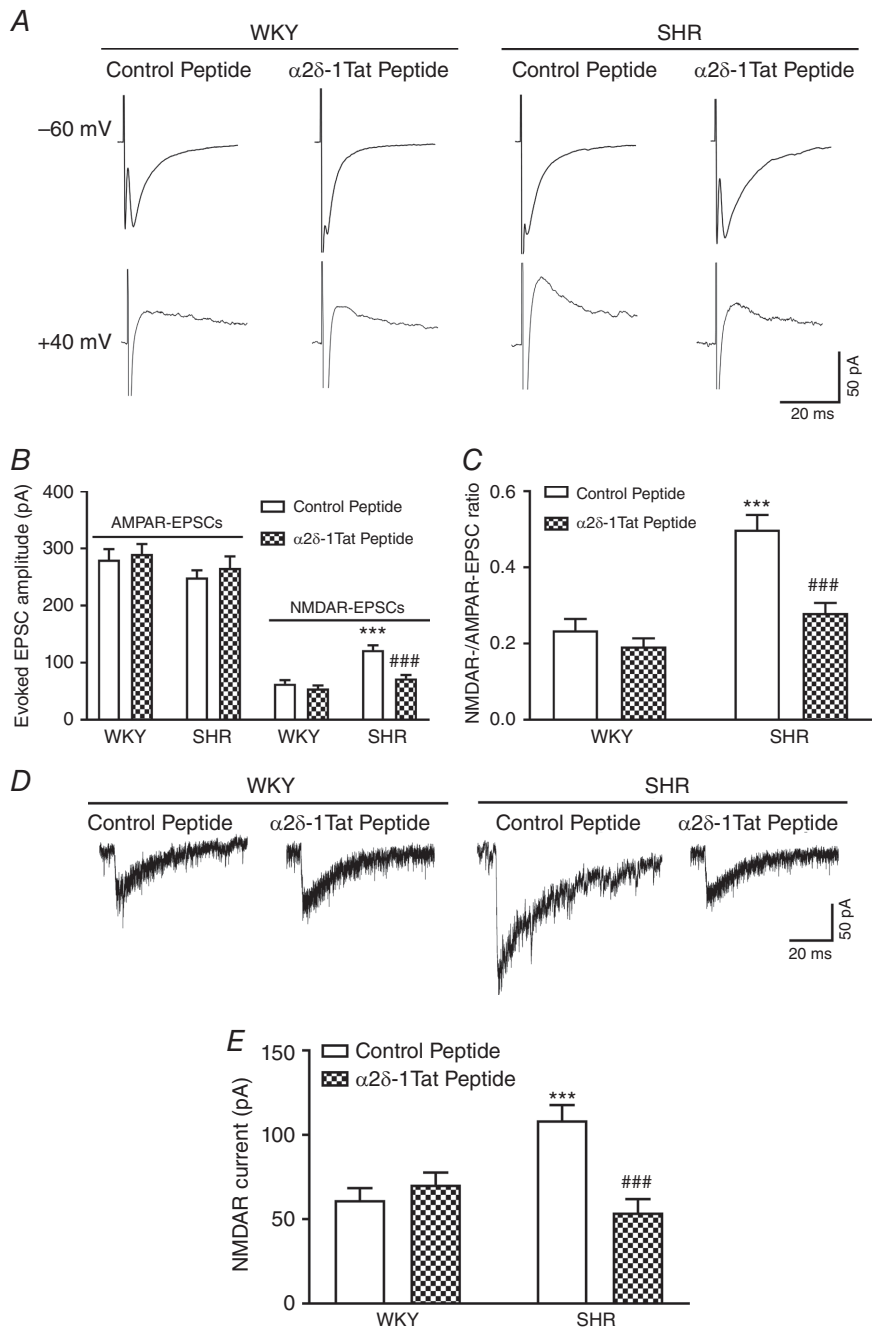


Figure 3. $\alpha 2\delta$ -1-bound NMDARs are essential for enhanced postsynaptic NMDAR activity of PVN presympathetic neurons in SHRs

A, representative current traces of evoked AMPAR-EPSCs (at -60 mV) and NMDAR-EPSCs (at $+40$ mV) recorded in labelled PVN neurons treated with control peptide or $\alpha 2\delta$ -1Tat peptide ($1 \mu\text{mol L}^{-1}$) in slices from a WKY rat and an SHR. B and C, summary of evoked AMPAR-EPSC and NMDAR-EPSC data (B) and the ratio of NMDAR-EPSCs to AMPAR-EPSCs (C) in labelled PVN neurons pretreated with control peptide or $\alpha 2\delta$ -1Tat peptide in slices from WKY rats ($n = 10$ neurons in each group) or SHRs ($n = 9$ neurons in each group). D and E, original current traces (D) and mean data (E) show the effect of $1 \mu\text{mol L}^{-1}$ control peptide or $1 \mu\text{mol L}^{-1}$ $\alpha 2\delta$ -1Tat peptide on puff NMDA ($100 \mu\text{mol L}^{-1}$) elicited currents of labelled PVN neurons recorded from WKY rats ($n = 8$ neurons in each group) and SHRs ($n = 11$ neurons in each group). $***P < 0.001$ compared to the WKY + control peptide group. $###P < 0.001$ compared to the SHR + control peptide group.

$\alpha 2\delta$ -1-bound NMDARs mediate increased synaptic glutamate release to PVN presympathetic neurons in SHRs

We next used $\alpha 2\delta$ -1Tat peptide to determine whether $\alpha 2\delta$ -1-bound NMDARs are responsible for the increased presynaptic NMDAR activity in SHRs. Pretreatment with $\alpha 2\delta$ -1Tat peptide ($1 \mu\text{mol L}^{-1}$, 60 min) completely

normalized the baseline frequency of mEPSCs of labelled PVN neurons in SHRs to the level in WKY rats (SHR + control peptide, $n = 9$ neurons; SHR + $\alpha 2\delta$ -1Tat peptide, $n = 10$ neurons) (Fig. 5A–E). However, $\alpha 2\delta$ -1Tat peptide had no effect on the frequency or amplitude of mEPSCs in WKY rats. After treatment with $\alpha 2\delta$ -1Tat peptide, further application of AP5 ($50 \mu\text{mol L}^{-1}$) no longer had any effect on mEPSCs of labelled PVN neurons

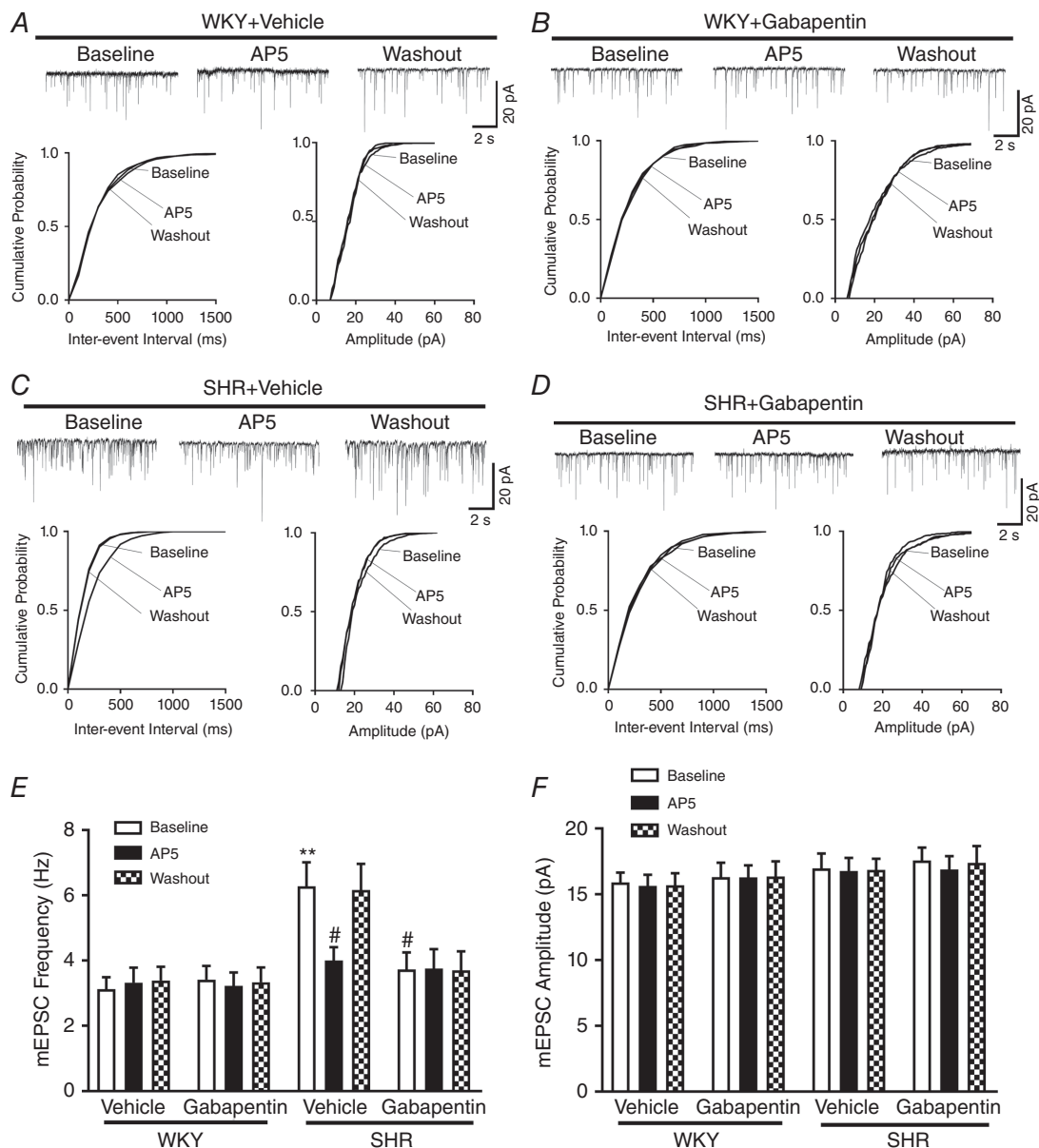


Figure 4. $\alpha 2\delta$ -1 mediates increased presynaptic NMDAR activity of RVLN-projecting PVN neurons in SHRs

A–D, original traces and cumulative probability plots show the effect of bath application of $50 \mu\text{mol L}^{-1}$ AP5 on the frequency and amplitude of mEPSCs of labelled PVN neurons pretreated with vehicle or $100 \mu\text{mol L}^{-1}$ gabapentin in slices from WKY rats and SHRs. E and F, summary data show the effects of gabapentin and AP5 on the frequency (E) and amplitude (F) of mEPSCs in labelled PVN neurons from WKY rats (vehicle, $n = 10$ neurons; gabapentin, $n = 12$ neurons) and SHRs ($n = 11$ neurons in each group). ** $P < 0.01$ compared to baseline in the WKY + vehicle group. # $P < 0.05$ compared to baseline in the SHR + vehicle group.

in brain slices from SHR (Fig. 5D–E). Treatment with the Tat-fused control peptide had no effect on the frequency or amplitude of mEPSCs of labelled PVN neurons in brain slices from WKY rats ($n = 12$ neurons) or SHR ($n = 9$

neurons) (Fig. 5A, C, E and F). These data indicate that $\alpha 2\delta$ -1-bound NMDARs are required for tonic activation of presynaptic NMDARs of PVN presympathetic neurons in SHR.

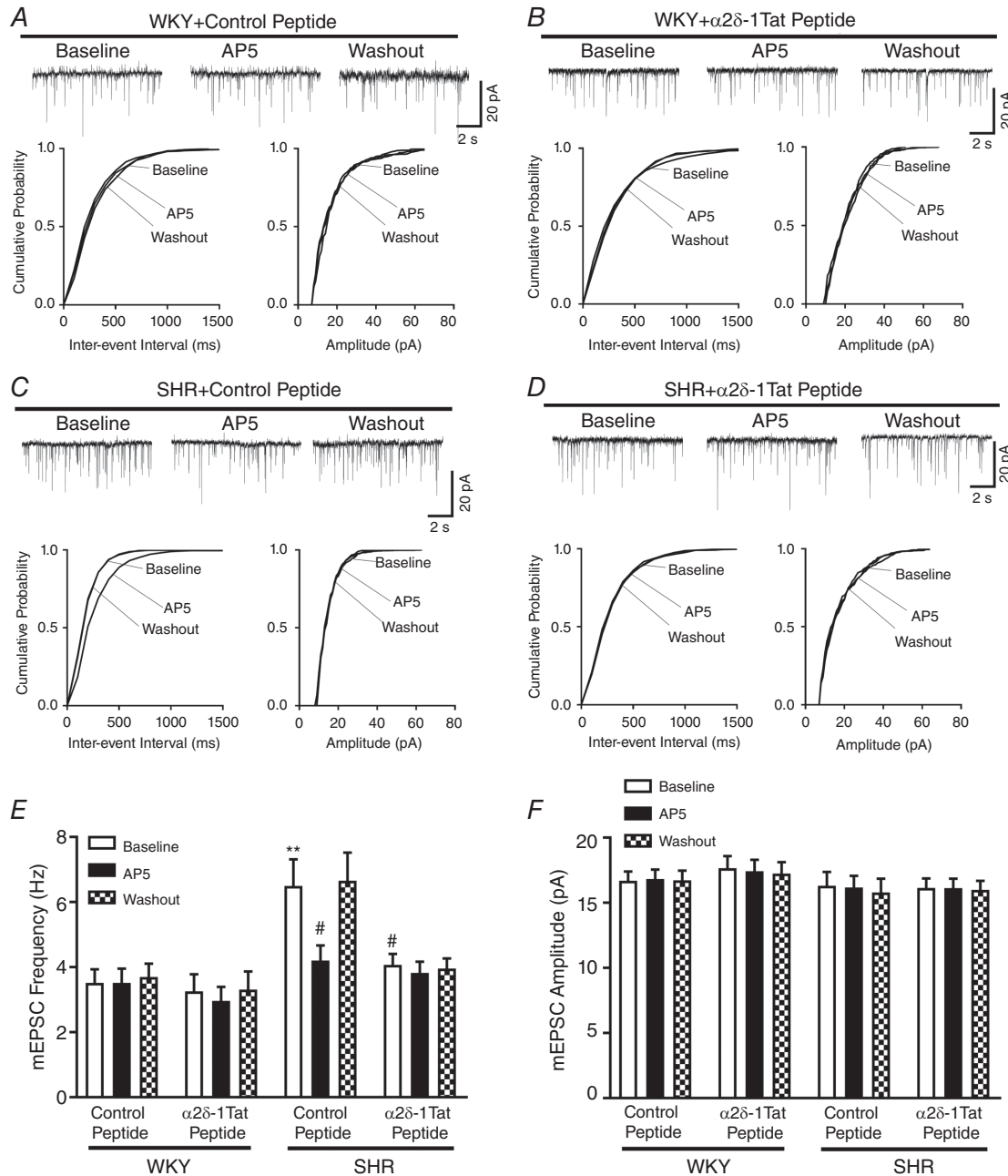


Figure 5. $\alpha 2\delta$ -1-bound NMDARs are essential for tonic activation of presynaptic NMDAR of PVN presympathetic neurons in SHR

A–D, original traces and cumulative probability plots show the effect of bath application of 50 $\mu\text{mol L}^{-1}$ AP5 on mEPSCs of labelled PVN neurons pretreated with 1 $\mu\text{mol L}^{-1}$ control peptide or 1 $\mu\text{mol L}^{-1}$ $\alpha 2\delta$ -1Tat peptide in slices from WKY rats and SHR. E and F, group data show the effects of $\alpha 2\delta$ -1Tat peptide and AP5 on the frequency (E) and amplitude (F) of mEPSCs in labelled PVN neurons from WKY rats (control peptide, $n = 12$ neurons; $\alpha 2\delta$ -1Tat peptide, $n = 11$ neurons) and SHR (control peptide, $n = 9$ neurons; $\alpha 2\delta$ -1Tat peptide, $n = 10$ neurons). ** $P < 0.01$ compared to baseline in the WKY + control peptide group. # $P < 0.05$ compared to baseline in the SHR + control peptide group.

$\alpha 2\delta$ -1-bound NMDARs in the PVN maintain heightened sympathetic vasomotor tone in SHR

Because gabapentin and pregabalin bind to both $\alpha 2\delta$ -1 and $\alpha 2\delta$ -2 (Gee *et al.* 1996; Gong *et al.* 2001; Marais *et al.* 2001; Li *et al.* 2011), we used $\alpha 2\delta$ -1Tat peptide to determine whether $\alpha 2\delta$ -1-bound NMDARs in the PVN play a role in heightened sympathetic vasomotor tone in SHR. We have shown previously that microinjection of AP5 into the PVN has no effect on the basal sympathetic vasomotor activity in normotensive WKY rats (Li & Pan, 2007). Microinjection of $\alpha 2\delta$ -1Tat peptide (50 pmol, 50 nL) bilaterally into the PVN significantly decreased the ABP ($P < 0.0001$, $F_{2,24} = 15.67$) and RSNA ($P < 0.0001$, $F_{2,24} = 20.20$) in SHR ($n = 9$ rats) (Fig. 6A–C). The effect of $\alpha 2\delta$ -1Tat peptide on the mean ABP and RSNA lasted for more than 60 min. In SHR microinjected with $\alpha 2\delta$ -1Tat peptide, subsequent microinjection of AP5 (1.0 nmol, 50 nL) (Li & Pan, 2007; Li *et al.* 2017; Qiao *et al.* 2017) into the PVN failed to further decrease ABP

and RSNA (Fig. 6A–C). By contrast, AP5 microinjection into the PVN significantly decreased ABP and RSNA in the SHR subjected to a prior microinjection of Tat-fused control peptide (50 pmol, 50 nL; $n = 9$ rats) (Fig. 6). These results suggest that $\alpha 2\delta$ -1-bound NMDARs in the PVN contribute to maintaining elevated sympathetic vasomotor tone in SHR.

Discussion

The present study reveals that the direct interaction between $\alpha 2\delta$ -1 and NMDARs in the brain is of high pathophysiological relevance in dysregulation of the autonomic nervous system in hypertension. We showed that the $\alpha 2\delta$ -1 protein level in the PVN was upregulated in SHR and that this increase in $\alpha 2\delta$ -1 was not altered by lowering ABP. These findings suggest that $\alpha 2\delta$ -1 upregulation in the PVN is not a secondary response to increased ABP in SHR but instead may contribute to

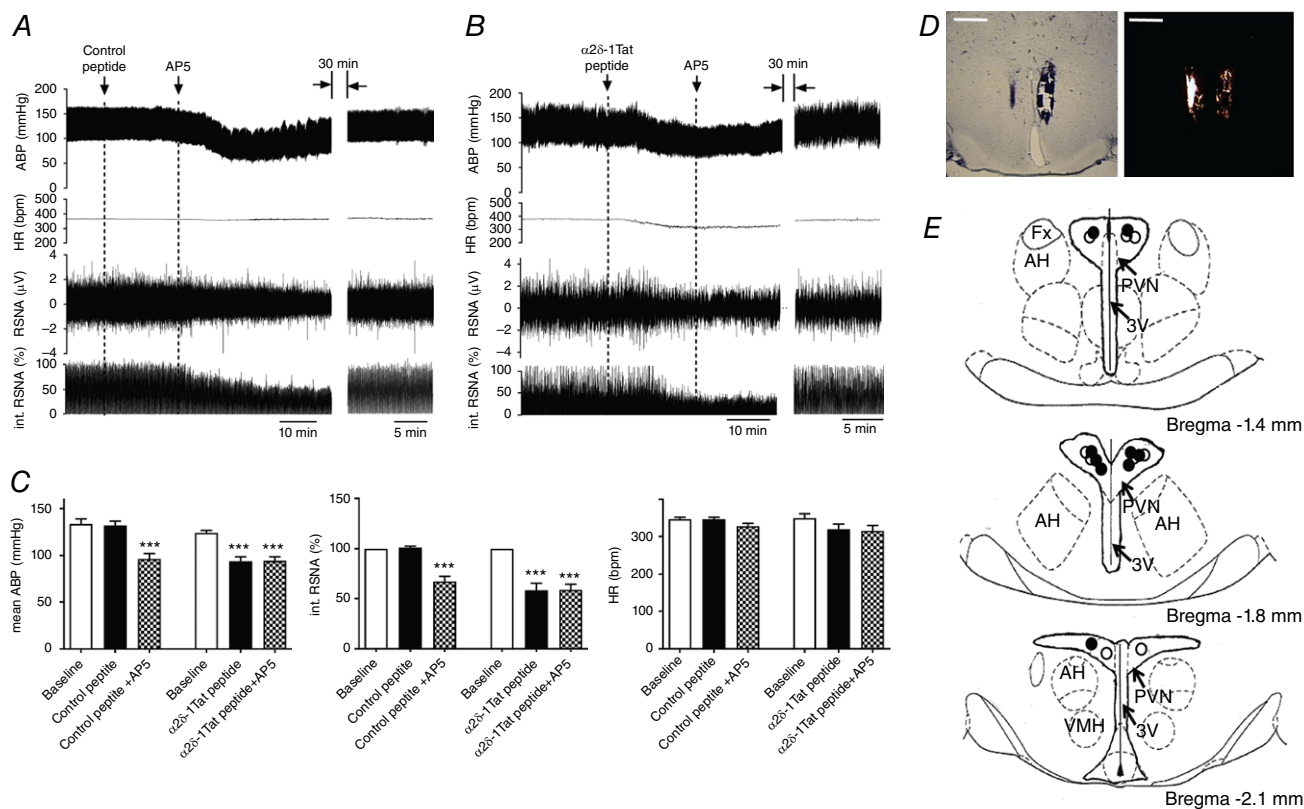


Figure 6. $\alpha 2\delta$ -1-bound NMDARs in the PVN maintain heightened sympathetic outflow in SHR

A and B, original recording traces show the effects of bilateral microinjection of control peptide (A) or $\alpha 2\delta$ -1Tat peptide (B) followed by AP5 microinjection into the PVN on ABP, RSNA and HR in SHR. C, summary data show changes in mean ABP, integrated RSNA (int. RSNA) and HR in response to microinjection of AP5 after microinjection of control peptide or $\alpha 2\delta$ -1Tat peptide into the PVN in SHR ($n = 9$ rats in each group). D and E, representative tissue section images (D) and schematic drawing (E) show the microinjection sites for control peptide plus AP5 (solid circle) and $\alpha 2\delta$ -1Tat peptide plus AP5 (open circle) in the PVN in SHR. *** $P < 0.001$ compared to the baseline control. 3V, third ventricle; AH, anterior hypothalamus; Fx, fornix; VMH, ventromedial hypothalamus. Scale bars = 1 mm. [Colour figure can be viewed at wileyonlinelibrary.com]

hypertension development. Consistent with this notion, we found that the $\alpha 2\delta$ -1 protein level in the PVN was significantly higher in 4-week-old prehypertensive SHR than in age-matched WKY rats. In the spinal cord, nerve injury-induced $\alpha 2\delta$ -1 upregulation promotes its interaction with NMDARs and the synaptic expression of $\alpha 2\delta$ -1-bound NMDARs (Chen *et al.* 2018). Consistent with this concept is our finding in the present study that $\alpha 2\delta$ -1 interacted with NMDARs in the hypothalamus and that the physical association between $\alpha 2\delta$ -1 and NMDARs was enhanced in SHRs. In addition, we show that the protein level of $\alpha 2\delta$ -1 and NMDARs in the hypothalamic synaptosomes was substantially increased in SHRs. Taken together, these biochemical data suggest that the prevalence of $\alpha 2\delta$ -1-bound NMDARs in the hypothalamus is increased in SHRs, which potentiates the synaptic trafficking of $\alpha 2\delta$ -1-NMDAR complexes in this hypertension model.

A major finding of the present study is that $\alpha 2\delta$ -1 is required for the increased presynaptic and postsynaptic NMDAR activity in PVN presympathetic neurons in SHRs. In the present study, we found unexpectedly that inhibiting $\alpha 2\delta$ -1 activity with gabapentin or disrupting the $\alpha 2\delta$ -1-NMDAR association with $\alpha 2\delta$ -1Tat peptide completely blocked the increased postsynaptic NMDAR

activity and NMDAR-mediated synaptic glutamate release to RVLM-projecting PVN neurons in SHRs. By contrast, gabapentin and $\alpha 2\delta$ -1Tat peptide had no effect on presynaptic or postsynaptic NMDAR activity of PVN presympathetic neurons in normotensive rats. The preferential effect of gabapentin and $\alpha 2\delta$ -1Tat peptide on synaptic NMDAR activity in SHRs is probably a result of the low $\alpha 2\delta$ -1 expression level in the PVN in normotensive rats. In support of this view, we have shown, in a heterologous expression system, that gabapentin inhibits NMDAR activity only when $\alpha 2\delta$ -1 is coexpressed (Chen *et al.* 2018). Our present findings indicate that $\alpha 2\delta$ -1-bound NMDARs account for most, if not all, of the increased synaptic NMDAR activity of PVN presympathetic neurons in SHRs. In addition to promoting synaptic trafficking of NMDARs, $\alpha 2\delta$ -1 can potentiate the NMDAR activity by reducing the voltage-dependent Mg^{2+} block of GluN2A-containing NMDARs (Chen *et al.* 2018).

The present study provides further evidence that $\alpha 2\delta$ -1 primarily functions as a critically important regulator of NMDARs in the central nervous system. Because we recorded mEPSCs and puff NMDA currents at a hold potential of -60 mV and in the presence of tetrodotoxin, VACCs are in a closed state in this recording condition. Therefore, $\alpha 2\delta$ -1 probably enhances the synaptic NMDAR

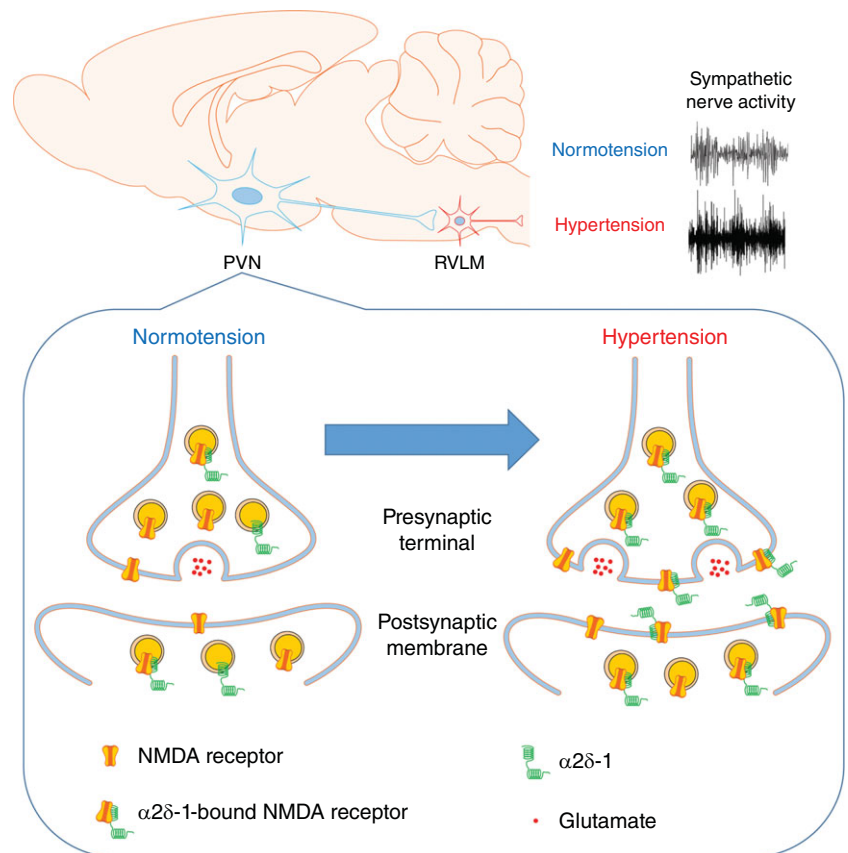


Figure 7. Schematic representation shows the proposed role of $\alpha 2\delta$ -1 in the regulation of synaptic NMDARs of PVN presympathetic neurons and sympathetic outflow in SHRs

In normotensive condition, most NMDARs are not associated with $\alpha 2\delta$ -1 in the PVN. In hypertensive condition, $\alpha 2\delta$ -1 is upregulated and physically interacts with NMDARs to promote synaptic trafficking of $\alpha 2\delta$ -1-bound NMDARs, which leads to increased pre- and postsynaptic NMDAR activity of RVLM-projecting PVN neurons. The increased synaptic NMDAR activity in the PVN contributes to elevated sympathetic vasomotor activity in SHRs. [Colour figure can be viewed at wileyonlinelibrary.com]

activity of PVN presympathetic neurons independent of VACCs. $\alpha 2\delta$ -1 may have a minor role in regulating VACC activity because $\alpha 2\delta$ -1 has a weak interaction with the pore-forming VACC $\alpha 1$ subunit in the brain (Muller *et al.* 2010). Furthermore, removing $\alpha 2\delta$ -1 has little effect on the overall VACC activity in cell lines and in hypothalamic neurons (Wu *et al.* 2009; Felsted *et al.* 2017). Previous studies have shown that protein kinases, such as casein kinase 2, calcium/calmodulin-dependent protein kinase II and Src kinases, contribute to the NMDAR hyperactivity of PVN presympathetic neurons in SHR (Ye *et al.* 2012b; Li *et al.* 2017; Qiao *et al.* 2017). However, the link between $\alpha 2\delta$ -1-bound NMDARs and protein kinases in regulating NMDAR activity in hypertension is currently unknown. Because increased phosphorylation can strengthen protein-protein binding complexes (Nishi *et al.* 2011), it is possible that certain protein kinases potentiate phosphorylation of $\alpha 2\delta$ -1 and/or NMDAR proteins to promote their physical interactions by changing their physicochemical properties, stability and dynamics.

The increased NMDAR activity in the PVN plays a dominant role in maintaining elevated sympathetic outflow in SHR (Li & Pan, 2007; Ye *et al.* 2011; Qiao *et al.* 2017). Our findings showing that $\alpha 2\delta$ -1-bound NMDARs in the PVN critically contributed to the increased synaptic NMDAR activity of PVN presympathetic neurons in SHR prompted us to determine the role of $\alpha 2\delta$ -1-bound NMDARs in the control of sympathetic outflow in hypertension. Consistent with our slice recording data is our finding that disrupting the $\alpha 2\delta$ -1-NMDAR interaction in the PVN substantially decreased ABP and RSNA in SHR. Importantly, subsequent microinjection of the NMDAR antagonist did not further decrease ABP and RSNA after pretreatment with $\alpha 2\delta$ -1Tat peptide in SHR. These results provide *in vivo* evidence that $\alpha 2\delta$ -1-bound NMDARs in the PVN are critically involved in sustaining elevated sympathetic vasomotor activity in the hypertensive condition.

In summary, we present substantial new evidence indicating that $\alpha 2\delta$ -1 plays a pivotal role in increased presynaptic and postsynaptic NMDAR activity of PVN presympathetic neurons and that $\alpha 2\delta$ -1-bound NMDARs in the PVN are required for maintaining sympathetic vasomotor tone in SHR (Fig. 7). Our study provides new insight into the molecular mechanism underlying elevated sympathetic outflow in an animal model of essential hypertension. Further studies are needed to determine whether $\alpha 2\delta$ -1-bound NMDARs play a role in autonomic dysregulation in other animal models of hypertension. Because neither gabapentin, nor $\alpha 2\delta$ -1Tat peptide affects the basal $\alpha 2\delta$ -1-free NMDARs, targeting $\alpha 2\delta$ -1-bound NMDARs could minimize the adverse effects associated with blocking physiological

NMDARs by general NMDAR antagonists. Some clinical studies suggest that gabapentinoids can reduce the pressor response elicited by tracheal intubation and the paroxysmal sympathetic hyperactivity caused by brain injury (Fassoulaki *et al.* 2006; Choi *et al.* 2013; Doleman *et al.* 2016). On the basis of our findings, $\alpha 2\delta$ -1-bound NMDARs could be targeted as a treatment for neurogenic hypertension.

References

- Allen AM (2002). Inhibition of the hypothalamic paraventricular nucleus in spontaneously hypertensive rats dramatically reduces sympathetic vasomotor tone. *Hypertension* **39**, 275–280.
- Chen J, Li L, Chen SR, Chen H, Xie JD, Sirrieh RR, MacLean DM, Zhang Y, Zhou MH, Jayaraman V & Pan HL (2018). The $\alpha 2\delta$ -1-NMDA receptor complex is critically involved in neuropathic pain development and gabapentin therapeutic actions. *Cell Rep* **22**, 2307–2321.
- Choi HA, Jeon SB, Samuel S, Allison T & Lee K (2013). Paroxysmal sympathetic hyperactivity after acute brain injury. *Curr Neurol Neurosci Rep* **13**, 370.
- Cole RL, Lechner SM, Williams ME, Prodanovich P, Bleicher L, Varney MA & Gu G (2005). Differential distribution of voltage-gated calcium channel α -2 delta subunit mRNA-containing cells in the rat central nervous system and the dorsal root ganglia. *J Comp Neurol* **491**, 246–269.
- DiBona GF (2013). Sympathetic nervous system and hypertension. *Hypertension* **61**, 556–560.
- Doleman B, Sherwin M, Lund JN & Williams JP (2016). Gabapentin for the hemodynamic response to intubation: systematic review and meta-analysis. *Can J Anaesth* **63**, 1042–1058.
- Fassoulaki A, Melemeni A, Paraskeva A & Petropoulos G (2006). Gabapentin attenuates the pressor response to direct laryngoscopy and tracheal intubation. *Br J Anaesth* **96**, 769–773.
- Felsted JA, Chien CH, Wang D, Panessiti M, Ameroso D, Greenberg A, Feng G, Kong D & Rios M (2017). $\alpha 2\delta$ -1 in SF1(+) neurons of the ventromedial hypothalamus is an essential regulator of glucose and lipid homeostasis. *Cell Rep* **21**, 2737–2747.
- Fuller-Bicer GA, Varadi G, Koch SE, Ishii M, Bodi I, Kadeer N, Muth JN, Mikala G, Petrashevskaya NN, Jordan MA, Zhang SP, Qin N, Flores CM, Isaacsohn I, Varadi M, Mori Y, Jones WK & Schwartz A (2009). Targeted disruption of the voltage-dependent calcium channel $\alpha 2\delta$ -1 subunit. *Am J Physiol Heart Circ Physiol* **297**, H117–H124.
- Gee NS, Brown JP, Dissanayake VU, Offord J, Thurlow R & Woodruff GN (1996). The novel anticonvulsant drug, gabapentin (Neurontin), binds to the $\alpha 2\delta$ subunit of a calcium channel. *J Biol Chem* **271**, 5768–5776.
- Gong HC, Hang J, Kohler W, Li L & Su TZ (2001). Tissue-specific expression and gabapentin-binding properties of calcium channel $\alpha 2\delta$ subunit subtypes. *J Membr Biol* **184**, 35–43.

- Hamer DW & Santer RM (1981). Anatomy and blood supply of the coeliac-superior mesenteric ganglion complex of the rat. *Anat Embryol (Berl)* **162**, 353–362.
- Li DP, Atnip LM, Chen SR & Pan HL (2005). Regulation of synaptic inputs to paraventricular-spinal output neurons by $\alpha 2$ adrenergic receptors. *J Neurophysiol* **93**, 393–402.
- Li DP, Chen SR & Pan HL (2003). Angiotensin II stimulates spinally projecting paraventricular neurons through presynaptic disinhibition. *J Neurosci* **23**, 5041–5049.
- Li DP & Pan HL (2006). Plasticity of GABAergic control of hypothalamic presympathetic neurons in hypertension. *Am J Physiol Heart Circ Physiol* **290**, H1110–H1119.
- Li DP & Pan HL (2007). Glutamatergic inputs in the hypothalamic paraventricular nucleus maintain sympathetic vasomotor tone in hypertension. *Hypertension* **49**, 916–925.
- Li DP, Yang Q, Pan HM & Pan HL (2008). Pre- and postsynaptic plasticity underlying augmented glutamatergic inputs to hypothalamic presympathetic neurons in spontaneously hypertensive rats. *J Physiol* **586**, 1637–1647.
- Li DP, Zhou JJ, Zhang J & Pan HL (2017). CaMKII regulates synaptic NMDA receptor activity of hypothalamic presympathetic neurons and sympathetic outflow in hypertension. *J Neurosci* **37**, 10690–10699.
- Li Z, Taylor CP, Weber M, Piechan J, Prior F, Bian F, Cui M, Hoffman D & Donevan S (2011). Pregabalin is a potent and selective ligand for $\alpha(2)\delta$ -1 and $\alpha(2)\delta$ -2 calcium channel subunits. *Eur J Pharmacol* **667**, 80–90.
- Marais E, Klugbauer N & Hofmann F (2001). Calcium channel $\alpha(2)\delta$ subunits-structure and gabapentin binding. *Mol Pharmacol* **59**, 1243–1248.
- Muller CS, Haupt A, Bildl W, Schindler J, Knaus HG, Meissner M, Rammner B, Striessnig J, Flockerzi V, Fakler B & Schulte U (2010). Quantitative proteomics of the Cav2 channel nano-environments in the mammalian brain. *Proc Natl Acad Sci U S A* **107**, 14950–14957.
- Nishi H, Hashimoto K & Panchenko AR (2011). Phosphorylation in protein-protein binding: effect on stability and function. *Structure* **19**, 1807–1815.
- Oparil S, Zaman MA & Calhoun DA (2003). Pathogenesis of hypertension. *Ann Intern Med* **139**, 761–776.
- Qiao X, Zhou JJ, Li DP & Pan HL (2017). Src kinases regulate glutamatergic input to hypothalamic presympathetic neurons and sympathetic outflow in hypertension. *Hypertension* **69**, 154–162.
- Reboussin DM, Allen NB, Griswold ME, Guallar E, Hong Y, Lackland DT, Miller EPR 3rd, Polonsky T, Thompson-Paul AM & Vupputuri S (2017). Systematic Review for the 2017 ACC/AHA/AAPA/ABC/ACPM/AGS/APhA/ASH/ASPC/NMA/PCNA Guideline for the Prevention, Detection, Evaluation, and Management of High Blood Pressure in Adults: A Report of the American College of Cardiology/American Heart Association Task Force on Clinical Practice Guidelines. *Hypertension*, <https://doi.org/10.1016/j.jacc.2017.1011.1004>
- Rock DM, Kelly KM & Macdonald RL (1993). Gabapentin actions on ligand- and voltage-gated responses in cultured rodent neurons. *Epilepsy Res* **16**, 89–98.
- Schumacher TB, Beck H, Steinhauser C, Schramm J & Elger CE (1998). Effects of phenytoin, carbamazepine, and gabapentin on calcium channels in hippocampal granule cells from patients with temporal lobe epilepsy. *Epilepsia* **39**, 355–363.
- Sulzer D & Pothos EN (2000). Regulation of quantal size by presynaptic mechanisms. *Rev Neurosci* **11**, 159–212.
- Taylor CP & Garrido R (2008). Immunostaining of rat brain, spinal cord, sensory neurons and skeletal muscle for calcium channel $\alpha(2)$ - $\delta(1)$ type 1 protein. *Neuroscience* **155**, 510–521.
- Wu ZZ, Li DP, Chen SR & Pan HL (2009). Aminopyridines potentiate synaptic and neuromuscular transmission by targeting the voltage-activated calcium channel β subunit. *J Biol Chem* **284**, 36453–36461.
- Ye ZY, Li DP, Byun HS, Li L & Pan HL (2012a). NKCC1 upregulation disrupts chloride homeostasis in the hypothalamus and increases neuronal activity-sympathetic drive in hypertension. *J Neurosci* **32**, 8560–8568.
- Ye ZY, Li DP, Li L & Pan HL (2011). Protein kinase CK2 increases glutamatergic input in the hypothalamus and sympathetic vasomotor tone in hypertension. *J Neurosci* **31**, 8271–8279.
- Ye ZY, Li L, Li DP & Pan HL (2012b). Casein kinase 2-mediated synaptic GluN2A up-regulation increases N-methyl-D-aspartate receptor activity and excitability of hypothalamic neurons in hypertension. *J Biol Chem* **287**, 17438–17446.

Additional information

Competing interests

The authors declare that they have no competing interests.

Author contributions

HM, S-RC, HC, J-JZ and D-PL performed the experiments and analysed data. HM drafted and revised the manuscript. H-LP conceived and designed the study and edited the manuscript. All authors approved the final version of the manuscript submitted for publication.

Funding

This work was supported by the National Institutes of Health (Grants HL131161 and HL142133) and the N.G. and Helen T. Hawkins Endowment (to H-LP).